Applied Mechanics and Materials
ISSN: 1662-7482, Vol. 835, pp 649-653
doi:10.4028/www.scientific.net/AMM.835.649

Submitted: 2015-10-15
Revised: 2015-12-17
Accepted: 2016-01-26
Online: 2016-05-11

Dynamic behavior of cellular materials under combined shear-compression

Yuanyuan Ding[1, a], Shilong Wang[1, b], Zhijun Zheng[1, c*], Liming Yang[2, d], Jilin Yu[1, e]

[1]CAS Key Laboratory of Mechanical Behavior and Design of Materials, University of Science and Technology of China, Hefei 230026, PR China

[2]Mechanics and Materials Science Research Center, Ningbo University, Ningbo 315211, PR China

[a]yyding05@mail.ustc.edu.cn, [b] long2012@mail.ustc.edu.cn, [c]zjzheng@ustc.edu.cn, [d] yangliming@nbu.edu.cn, [e] jlyu@ustc.edu.cn.

Keywords: Cellular materials, Combined shear-compression, Finite element method, Dynamic behavior

Abstract. A 3D cell-based finite element model is employed to investigate the dynamic biaxial behavior of cellular materials under combined shear-compression. The biaxial behavior is characterized by the normal stress and shear stress, which could be determined directly from the finite element results. A crush plateau stress is introduced to illustrate the critical crush stress, and the result shows that the normal plateau stress declines with the increase of the shear plateau stress, which climbs with the increase of loading angle. An elliptical criterion of normal plateau stress vs. shear plateau stress is obtained by the nonlinear regression method.

Introduction

Cellular material, as an energy absorption material, has been employed in many fields, such as automotive, rail and aerospace industries [1]. Considering the diversity and complexity of actual load conditions for the cellular material, the dynamic multiaxial behavior should be investigated to guide the engineering design.

Under quasi-static loading rates, several multiaxial loading devices [2-5] were proposed to investigate the multiaxial behavior of cellular materials. Furthermore, different types of yield envelope of the cellular material were approximately depicted based on the quasi-static multiaxial tests. For example, Deshpande and Fleck [3] proposed an isotropic constitutive model for metallic foams based on the quadratic shape yield surface in the stress space of mean stress and effective stress.

Under dynamic loading rate, some simple multiaxial loading tests were also developed. Chung and Waas [6] carried out the dynamic multiaxial loading tests using a drop hammer test machine with the lateral displacement constrained. Yu et al. [7] performed a passive multiaxial test of aluminum foams by SHPB technique. Hong et al. [8] achieved the dynamic multiaxial data of aluminum honeycomb specimens by combined shear-compression tests. However, due to the complexity of the dynamic multiaxial loading devices and the invisibility of the deformation mode of specimens, the understanding of the mechanical behavior of metallic foams under multiaxial loading is limited.

In this paper, a dynamic combined shear-compression virtual test is presented and it provides the normal compression and shear behaviors of cellular materials, which could be employed to further investigate the yield criterion of cellular materials.

Material Models and Virtual Tests

Closed-cell foam models with a uniform cell-wall thickness are generated by using the 3D Voronoi technique, see Ref. [9] for details. The cell-wall material is assumed to be elastic, perfectly plastic with Young's modulus $E = 69$ GPa, Poisson's ratio $v = 0.3$, yield stress $Y = 170$ MPa and density $\rho_s =$

2700 kg/m^3. The cell walls of Voronoi structures are meshed with shell elements (types S3R and S4R). In this study, the relative density of the Voronoi structure is set as $\rho_0/\rho_s = 0.1$, where ρ_0 is the initial density of the Voronoi structures. Numerical simulations were performed by using the finite element code ABAQUS/Explicit. The macroscopic properties could be well simulated by using a Voronoi structure with at least five cells along the shortest length direction. Therefore, the cellular specimen used in this study is constructed in a volume of 20 × 20 × 20 mm^3 with 400 nuclei, and the corresponding average cell diameter is about 3.3 mm, as shown in Fig. 1(a).

A constant velocity virtual test under combined shear-compression is considered in this study. The cellular specimen is placed between two rigid plates, as depicted in Fig. 1(b). The left rigid plate is set as a fixed end and the right rigid plate is a loading plate with a constant velocity V at an angle of θ. In this model, a general contact with a friction coefficient of 0.02 is defined for the whole model except the interface between the loading plate and the cellular specimen, which is defined by the rough friction constrain to make sure no slip occurs.

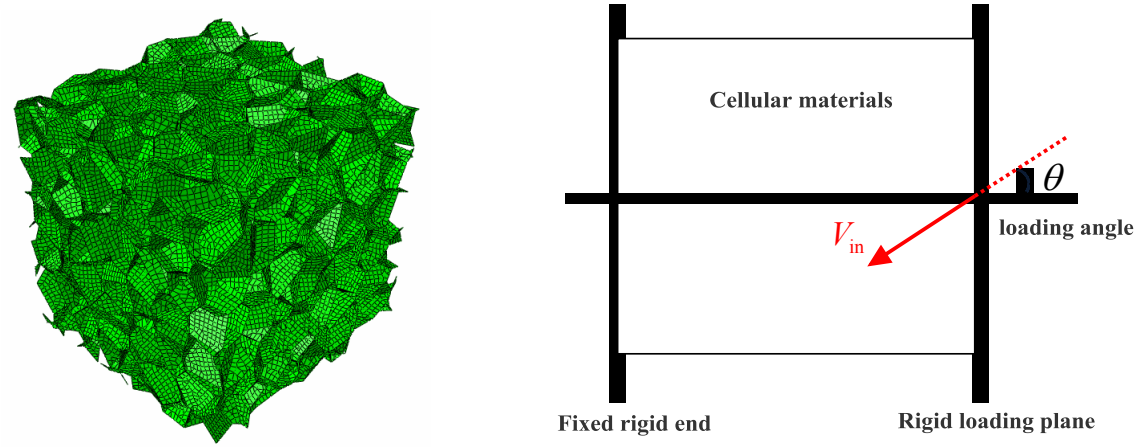

(a) (b)

Fig. 1 A cell-based finite element model (a) and its constant velocity impact scenario under combined shear-compression (b).

Results and Discussion

In this section, the combined shear-compression simulations with the loading angles of 15°, 30°, 45° and 60° under the constant input velocity V_{in} = 30 m/s are presented. The normal force F_n and the shear force F_s, which are the contact forces at the interface of cellular materials and loading plate, as shown in Fig. 2, could be directly obtained from numerical results. The overall crush displacement δ is determined by $V_{in} \times t$, where t is the loading time.

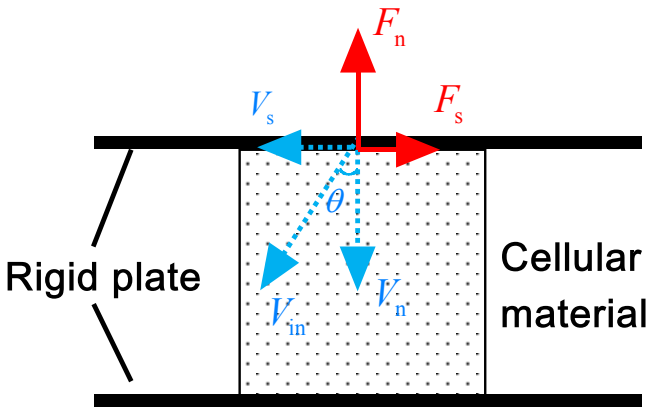

Fig. 2 Scheme of the decompositions of force and velocity.

By taking $\theta = 30°$ as an example, the normal stress and the shear stress are depicted in Fig. 3. It transpires that the normal and shear stress curves exhibit similar trends, which could be characterized as an initial crushing region and a plateau region. During the initial crushing stage, both stresses jump to the initial peak rapidly, which could be physically understood as the action of the elastic wave. During the second stage (plateau region), the stresses fall from the initial peak to the plateau stress, which are mainly controlled by the plastic collapse behavior of cells. Therefore, two characteristic stresses, namely the initial yield stress (initial peak) and plateau crush stress, are introduced. Generally, cellular materials are used for cushioning and energy absorption in engineering practice, so the plateau crush stress may be much significant. Here, we define the plateau crush stress as,

$$\sigma_{\mathrm{pl}} = \frac{1}{\delta_{\max} - \delta_{\mathrm{in}}} \int_{\delta_{\mathrm{in}}}^{\delta_{\max}} \sigma \mathrm{d}\delta \tag{1}$$

where, δ_{in} is the crush displacement corresponding to the initial peak, and $\delta_{\max}$ denotes the maximum crush displacement, beyond which the cellular specimen could flip down easily ($\delta_{\max}$ = 7 mm in this study).

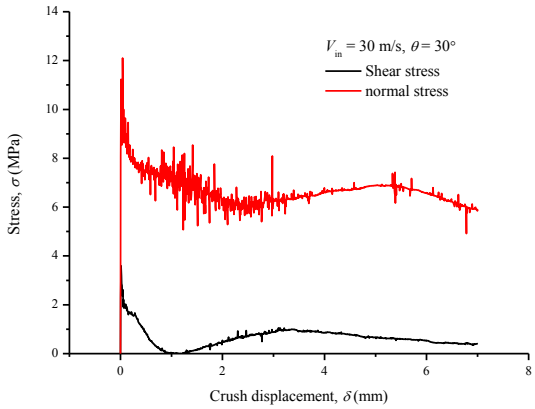

Fig. 3 Normal and shear stress curves at a velocity of 30 m/s with $\theta = 30°$.

The deformation patterns of the specimen under combined shear-compression with the loading angle 30° are shown in Fig. 4. As the loading plate moves from the original position to the down-left side as shown in Fig. 1(b), the cellular specimens incline during the crushing. At the beginning, the strip part in the cellular material, which is close to the loading plate, is first collapsed. Then a random shear band marked by the red circle appears in the cellular specimen as it is further loaded. It indicates that the shear band is a relatively weak band in the cellular material. The whole cellular specimen declines along the loading direction due to the friction force acting on the interfaces of the rigid plates and the specimen.

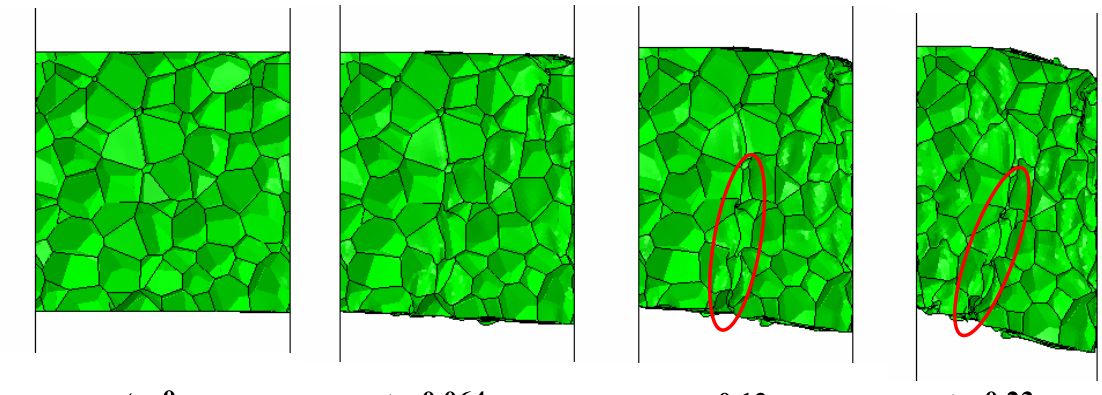

Fig. 4 Deformation configuration of cellular materials under dynamic combined shear-compression (V_{in} = 30 m/s, $\theta = 30°$).

Obviously, the normal stress and the shear stress are different when the loading angle changes. Three loading angles, $\theta = 0°$ (pure compression), 30° and 60°, are taken as examples to illustrate the change of normal stress and shear stress, as shown in Fig. 5. The level of normal stress curves decreases with the increase of loading angle, while the level of shear stress curves shows the opposite. The phenomena also match the practical cases [10].

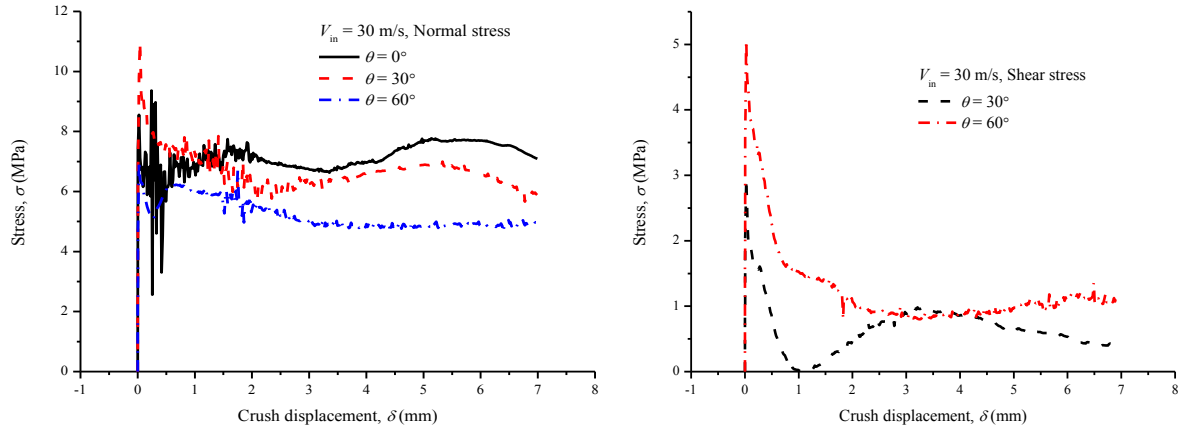

(a) (b)

Fig. 5 Normal compression (a) and shear (b) behaviors of cellular materials under dynamic combined shear-compression.

The plateau crush stresses of compression and shear calculated by Eq. (1) are shown in Fig. 6. Furthermore, the shear plateau stress-normal plateau stress states under dynamic combined shear-compression are depicted in Fig. 7. An elliptical shape is found for the crushing envelope, like that for honeycombs reported in Ref. [10], as;

$$\left(\frac{\sigma}{\sigma_0}\right)^2+\left(\frac{\tau}{\tau_0}\right)^2=1 \tag{2}$$

where, σ_0 and τ_0 are the normal plateau stress under uniaxial compression and the shear plateau stress under pure shear loading, respectively. By the method of nonlinear regression, the two material parameters could be determined as σ_0 = 7.12 MPa and τ_0 = 1.79 MPa in this study.

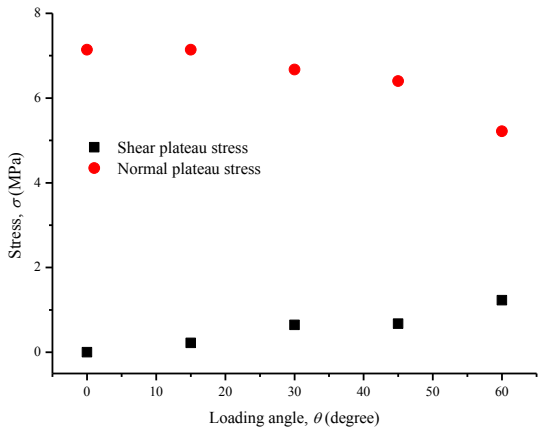

Fig. 6 The normal and shear plateau stresses at various loading angle.

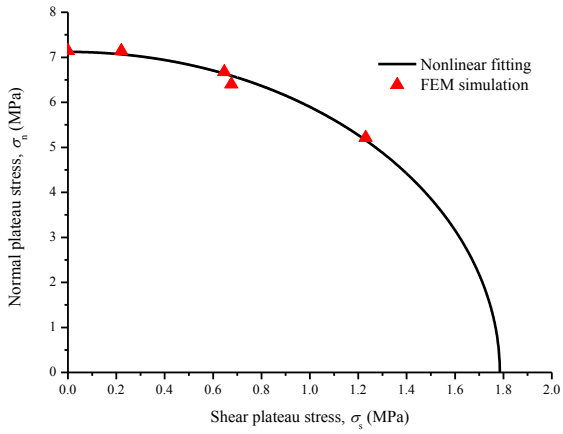

Fig. 7 Crush envelope of cellular materials in normal plateau stress vs. shear plateau stress.

Summary

In this paper, the dynamic biaxial behavior of cellular materials is investigated by virtual tests using a 3D Voronoi specimen. The specimen is loaded under combined shear-compression with

different loading angle at a constant velocity. The normal stress and the shear stress have been obtained from the numerical results. It is found that the level of compression strengths of cellular materials decreases with the increase of the loading angle, and the level of shear strengths varies in an opposite way. Two characteristic stresses, i.e. the initial peak stress and the plateau crush stress, are introduced to characterize the cushioning and energy absorption capability of cellular materials. The results reveal that under biaxial loading the envelope of normal plateau stress and shear plateau stress could be described with an elliptical criterion.

Acknowledgements

This work is supported by the National Natural Science Foundation of China (Project No. 11372308) and the Fundamental Research Funds for the Central Universities (Grant No. WK2480000001).

References

[1] L.J. Gibson, M.F. Ashby, Cellular solids: Structure and Properties, second ed., Cambridge, UK: Cambridge University Press, 1997.

[2] S.D. Papka, S. Kyriakides, Biaxial crushing of honeycombs-Part I: Experiments, Int. J. Solid. Struct. 36 (1999) 4367-4396.

[3] V.S. Deshpande, N.A. Fleck, Isotropic constitutive models for metallic foams, J. Mech. Phys. Solid. 48 (2000) 1253-1283.

[4] M. Doyoyo, T. Wierzbicki, Experimental studies on the yield behavior of ductile and brittle aluminum foams, Int. J. Plast. 19 (2003) 1195-1214.

[5] D. Ruan, G. Lu, L.S. Ong, B. Wang, Triaxial compression of aluminium foams, Compos. Sci. Technol. 67 (2007) 1218-1234.

[6] J. Chung, A.M. Waas, Compressive response of circular cell polycarbonate honeycombs under in plane biaxial static and dynamic loading. Part I: Experiments, Int. J. Impact Eng. 27 (2002) 729-754.

[7] J.L. Yu, E.H. Wang, J.R. Li, An experimental study on the quasi-static and dynamic behavior of aluminum foams under multi-axial compression, Adv. Heterogen. Mater. Mech. (2008) 879-882.

[8] S.T. Hong, J. Pan, T. Tyan, P. Prasad, Dynamic crush behaviors of aluminium honeycomb specimens under compression dominant inclined loads, Int. J. Plast. 24 (2008) 89-117.

[9] Z.J. Zheng, C.F. Wang, J.L. Yu, S.R. Reid, J.J. Harrigan, Dynamic stress-strain states for metal foams using a 3D cellular model, J. Mech. Phys. Solid. 72 (2014) 93-114.

[10] B. Hou, S. Pattofatto, Y.L. Li, H. Zhao, Impact behavior of honeycombs under combined shear-compression. Part II: Analysis, Int. J. Solid Struct. 48 (2011) 698-705.